Eletrochemical reduction of patulin and 5-hydroxymethylfurfural in both neutral and acid non-aqueous media. Their electroanalytical determination in apple juices

Gerardo Damián Chanique, Alejandro Heraldo Arévalo, María Alicia Zon*, Héctor Fernández*

Departamento de Química, Facultad de Ciencias Exactas, Físico-Químicas y Naturales, Universidad Nacional de Río Cuarto, Agencia Postal No 3,5800, Río Cuarto, Argentina

ABSTRACT

The electro-reduction of patulin mycotoxin and 5-hydroxymethylfurfural at glassy carbon electrodes in acetonitrile $+0.1 \, \mathrm{mol \, L^{-1}}$ tetrabutylammonium perchlorate, in both the absence and the presence of different aliquots of trifluoroacetic acid is reported. 5-hydroxymethylfurfural is the most common interference in the determination of patulin in products derived from apples. The electrochemical techniques were cyclic and square wave voltammetries, and controlled potential bulk electrolysis. The number of electrons exchanged in the patulin electro-reduction of $n=1$ could be inferred from controlled potential bulk electrolysis measurements. Ultraviolet-visible and infrared spectroscopies were used to identify patulin electro-reduction product/s. A value of $(2.1 \pm 0.1) \times 10^{-5} \, \mathrm{cm^2 \, s^{-1}}$ for the patulin diffusion coefficient was calculated from convoluted cyclic voltammograms. A method based on square wave voltammetry was developed for the quantitative determination of patulin in both fresh, and commercial apple juices in the presence of 5-hydroxymethylfurfural. Calibration curves obtained from solutions of the commercial reagent, and commercial apple juices were linear in the range from 3.0×10^{-7} to $2.2 \times 10^{-5} \, \mathrm{mol \, L^{-1}}$. The lowest concentration measured experimentally for a signal to noise ratio of 3:1 was $3 \times 10^{-7} \, \mathrm{mol \, L^{-1}}$ (45 ppb) and a recovery percent of 84% was determined for commercial apple juices. This electroanalytical methodology appears as a good screening method for the determination of patulin in apple juices.

© 2013 Elsevier B.V. All rights reserved.

1. Introduction

Patulin (4-hydroxy-4H-furo [3,2–c]pyran-2(6H)-one, PAT) is a mycotoxin produced by fungi belonging to several genera, including *Penicillium*, *Aspergillus*, and *Byssochlamys* [1]. PAT is an α, β-unsaturated-γ-lactone (Scheme 1). PAT has two conjugated double bonds, and a very reactive hemiacetal group, which racemizes quickly in aqueous media, precluding isolation of the (+) and (−) optical isomers [2].

The major sources of PAT contamination are apples with blue rot, cider, and juice pressed from moldy fruit. *Penicillium expansum* is considered the main producer of PAT in apple products [3]. However, PAT is sometimes found in other fruits such as pears, apricots, peaches, and grapes, being produced in the rotten parts of these fruits [4].

PAT has a low molecular weight and is soluble in water and polar organic solvents. It is not destroyed by heat and it is stable in acid medium, but unstable in an alkaline medium or by fermentation [1,5].

During the forties PAT was isolated as a broad-spectrum antifungal antibiotic. However, subsequent studies suggested that PAT not only was toxic to fungi and bacteria, but was also highly toxic to plant and animal cells. PAT can react with terminal sulfhydryl groups of proteins and polypeptides present in food [6]. PAT has mutagenic, genotoxic, immunotoxic, and neurotoxic effects on rodents [7] and teratogenic effects on chickens [8]. Exposure of humans to PAT via consumption of infected products may result in severe toxicosis, including mutagenic, teratogenic, hepatoxic, nephrotoxic, neurotoxic, and genotoxic effects. Its acute effects include nausea, vomiting, and other gastrointestinal traumas that accompany kidney damage [7,9,10]. At high doses, PAT exhibits immunosuppressive properties [11].

The International Agency for Research on Cancer (IARC) classifies PAT in the Group 3 (an agent not classifiable as carcinogenic to humans) [12].

The Food and Drug Administration of United States (FDA) has recommended an allowable maximum level of 50 ppb for fruit juices and their products [13], due to evidence of adverse effects of PAT. To date, no epidemiological or toxicological data have been published to indicate whether the consumption of PAT is

* Corresponding authors. Tel.: +54 358 467 6440; fax: +54 358 467 6233.
  E-mail addresses: azon@exa.unrc.edu.ar,
alicia_zon@hotmail.com (M. Alicia Zon), hfernandez@exa.unrc.edu.ar,
hfernandezster@gmail.com (H. Fernández).
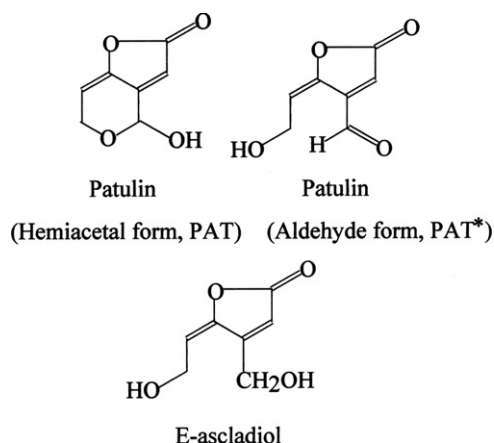
Scheme 1. Chemical structures of both patulin hemiacetal and aldehyde forms, and E-ascladiol.

dangerous to humans. However, there is an allowable level of PAT in apple products, considering that infants and young children are the major consumers of these foods, and effects of exposure to PAT for a long time are not still known [14,15].

The official method for determination of PAT is high performance liquid chromatography (HPLC) with ultraviolet (UV) detection, as is described by the Association of Official Analytical Chemistry (AOAC), item 995.10 [16,17]. The HPLC/UV or with a diode array detector (HPLC/DAD) [18] is also routinely used for quantitative determination of PAT in apple products. However, methods to confirm the presence of PAT usually include more specific detection techniques such as mass spectrometry (MS) after liquid chromatography (LC), gas chromatography (GC) separations [17,19], and high resolution gas chromatography/ high resolution mass spectrometry (HRGC/HRMS) [20]. Capillary electrophoresis is another technique to perform PAT determinations [21]. Analytical methods based on immunochemical technology are currently being investigated, but the low molecular weight of PAT presents a challenge for this area of research and development [10]. Therefore, the standard methodology to quantify PAT requires specific instrumentation and trained operators [10].

As far as we know, only one report related to the electrochemical reduction of PAT is found in the literature, with very little information [22]. On the other hand, Tanabe and Suzuki [23] reduced chemically the hemiacetal group of PAT to form E-ascladiol (Scheme 1), a compound reported to be 25% as toxic as PAT, although it has the same unsaturated bonds and γ lactone structure. In addition, it is well known that the PAT biosynthesis involves a series of condensation stages and redox reactions, several of which are catalyzed by enzymes. The E-ascladiol is involved in the last stage of PAT biosynthesis [11]. The E-ascladiol is either oxidized to PAT or non-enzymatically converted to its isomer Z-ascladiol.

On the other hand, the 5-hydroxymethylfurfural (HMF) is the most common interference in the determination of PAT in apple juices and derived products. Moreover, HMF is present at levels two or three times higher than PAT, which can cause a serious problem for the determination of PAT in natural samples [24].

In this study, we report results about the electro-reduction of PAT and HMF at glassy carbon (GC) electrodes in acetonitrile (ACN)+0.1 mol L^{-1} tetrabutylammonium perchlorate (TBAP), in the absence and in the presence of different aliquots of trifluoroacetic acid (TFA). The electrochemical techniques used were cyclic (CV) and square wave (SWV) voltammetries, and controlled potential bulk electrolysis. ACN+0.1 mol L^{-1} NaClO$_4$ was used as the reaction medium for performing measurements of controlled potential electrolysis. UV–vis and IR spectroscopies were used to

identify PAT electro-reduction product/s after performing controlled potential electrolysis. A method using SWV was developed for the quantitative determination of PAT in both fresh and commercial apple juices.

2. Experimental

2.1. Reagents

PAT, HMF and TFA were obtained from Sigma Chemical Company and used as received. ACN (Sintorgan, HPLC grade), was dried over molecular sieves of 3 Å for 48 h prior to use, and then used without further purification. TBAP was obtained from Fluka (electrochemical grade). It was dried under vacuum at 60 °C, and stored in desiccators. NaClO$_4$ (Merck p.a.) was recrystallized three times in water and dried under vacuum at 180 °C, and then stored in desiccators.

Stock solutions of PAT and HMF were prepared in ACN. They were stored at 8 °C in the dark. Working solutions were prepared daily by adding aliquots of stock solution to ACN+0.1 mol L^{-1} TBAP, in the absence and in the presence of different aliquots of TFA. PAT bulk concentration (c_{PAT}^{*}), and HMF bulk concentration (c_{HMF}^{*}) were varied from 3×10^{-7} to 1.4×10^{-3} mol L^{-1}, and from 3.4×10^{-4} to 2.3×10^{-3} mol L^{-1}, respectively.

Fresh apple juices were obtained from apples purchased at a local grocery store, choosing those blocks that had no signs of putrefaction by fungi. Juices were filtered using a glass fiber paper and were called "cloudy apple juices." We also analyzed commercial apple juices, called "clear apple juices." The difference between both juices is that the "clear apple juice" is subjected to a process of depectinization, clarification, and post-filtering; while these processes were not applied to the "cloudy apple juice". PAT extraction procedure was performed in triplicate following the AOAC official method [11,16,17,24]. The reproducibility relative standard deviations (RSDR) were of 20% and 14% for "cloudy apple juices" and "clear apple juice", respectively. Value for "clear apple juice" is close to those reported by Brause et al. for similar matrixes by HPLC [16]. Three extractions were performed using 5 mL of fresh and commercial apple juices with 10 mL of ethyl acetate. The three organic phases were collected in a separator funnel and purified with 2 mL of a 1.5% Na$_2$CO$_3$ solution. As it has been reported, the rate of decomposition of patulin depends on pH i. e. values for half-life ranged from 64 h at pH 8.0 to 1310 h at pH 6.0 [25]. Thus, the recommendation suggested by the International Standard ISO 8128-1 U.S.: 1993 [26] was considered, i.e. after combining the phases, the extraction was performed with Na$_2$CO$_3$ solution as quickly as possible, i.e. 1 min to 2 min. Then, a new extraction was performed with 5 mL of ethyl acetate. The ethyl acetate extract (35 mL) was dried using 1 g of anhydrous sodium sulfate. The solution was filtered through glass fiber paper and rinsed with 5 mL of ethyl acetate. Finally, the solvent was evaporated and the extract was re-dissolved in 5 mL of ACN+0.1 mol L^{-1} TBAP for analysis. Two procedures were used in the treatment of extracts: one was conducted on the juice as obtained and, the other; the juice was spiked with a known amount of PAT, i.e., 1.29×10^{-5} mol L^{-1}. We use the standard additions method to calculate the recovery percent.

2.2. Apparatus and experimental measurements

A conventional two-compartment glass cell was used for the voltammetric measurements. The working electrode was a GC disk of 3 mm dia. (Bioanalytical Systems). Before each measurement, it was polished successively with wet alumina powder (0.3 and 0.05 μm from Fischer), rinsed copiously with distilled water, sonicated in a

water bath for 2 min, and then dried. Its geometric area (A=0.083 cm^2) was determined by chronoamperometric measurements using 1.1×10^{-3} mol L^{-1} ferrocene (Fc)+ACN+0.1 mol L^{-1} tetrabutyl ammonium perchlorate (TBAP) through the Cottrell plots [27], using a value of 2.26×10^{-5} cm^2 s^{-1} for the Fc diffusion coefficient [28]. The counter electrode was a platinum foil of large area (A $\approx$ 2 cm^2). The reference electrode was an aqueous saturated calomel electrode (SCE), fitted with a fine-glass Luggin capillary containing a bridge solution identical to that of the sample which is measured.

Bulk-electrolysis glass cell was one of the tree-compartment type. A glass fiber paper held in place between the two halves separated the working and counter electrode compartments. The working electrode was a GC cylindrical bar of area 2.9 cm^2, which allowed a high speed continuous rotation. The counter electrode was a stainless foil of area 16 cm^2.

The reduction peak of PAT was strongly affected by dissolved oxygen in the medium. To avoid this effect, the presence of oxygen was minimized by purging with supporting electrolyte solution-saturated pure argon through the solution for about 20 min until the classical oxygen reduction peak, at about -1.0 V vs. SCE, disappeared. Then, the cell was kept under an argon atmosphere throughout experiments.

The measuring system for performing CV, SWV, chronoamperometry, and controlled potential bulk electrolysis was an AUTOLAB PGSTAT30 potentiostat (EcoChemie, The Netherland) run with the GPES (version 4.9) electrochemical analysis software. In CV, the scan rate was varied from 0.025 to 0.200 V s^{-1}. The characteristic SWV parameters were: amplitude (ΔE_{SW})=0.025 V, staircase step height (ΔE_s)=0.005 V, and the frequency (f) was varied from 10 Hz to 100 Hz.

Positive-feedback technique was employed in all experiments to compensate the solution resistance. In most of the cases, compensated solution resistance was about 100 Ω. The resistance determined represents approximately 90% of the value where the potentiostat instability was reached.

UV–vis absorption spectra were recorded using a Hewlett-Packard model 8452 A spectrophotometer, equipped with a temperature controller. Silica cells were of 1 cm path length. The absorbance values at λ=275 nm were obtained from spectra recorded against the corresponding blanks. Absorption spectra at different c^*_{PAT} in ACN were recorded. A plot of A^{ACN}_{275} vs. c^*_{PAT} was linear from 5.9×10^{-6} to 6.5×10^{-5} mol L^{-1}. The molar extinction coefficient was ε^{ACN}_{275}=$(1.65 \pm 0.02) \times 10^4$ mol^{-1} L cm^{-1}. The IR spectra were obtained from a Nicolet spectrophotometer, Impact 400 model. All the experiments were performed at 25 ± 0.2 °C.

3. Results and discussion

3.1. Neutral medium

3.1.1. Voltammetric measurements

A typical cyclic voltammogram of PAT at a GC electrode in ACN+0.1 mol L^{-1} TBAP, after subtraction of blank currents, is shown in Fig. 1a. PAT shows an only one reduction irreversible peak centered at about -1.56 V vs. SCE. This reduction peak is stable and reproducible if the potential is maintained for 30 s at 1.650 V before the potential sweep. No complementary anodic peak was observed when the sweep direction was reversed, clearly showing a PAT complex electro-reduction mechanism.

Plots of cathodic peak current ($I_{p,c}$) vs. v$^{1/2}$ were linear, indicating that the electrode process is diffusion controlled [27].

In addition, plots of the cathodic peak potential ($E_{p,c}$) vs. log v, and $E_{p,c}$ vs. log c^*_{PAT} were linear, with slopes of–(0.035 ± 0.001) V/
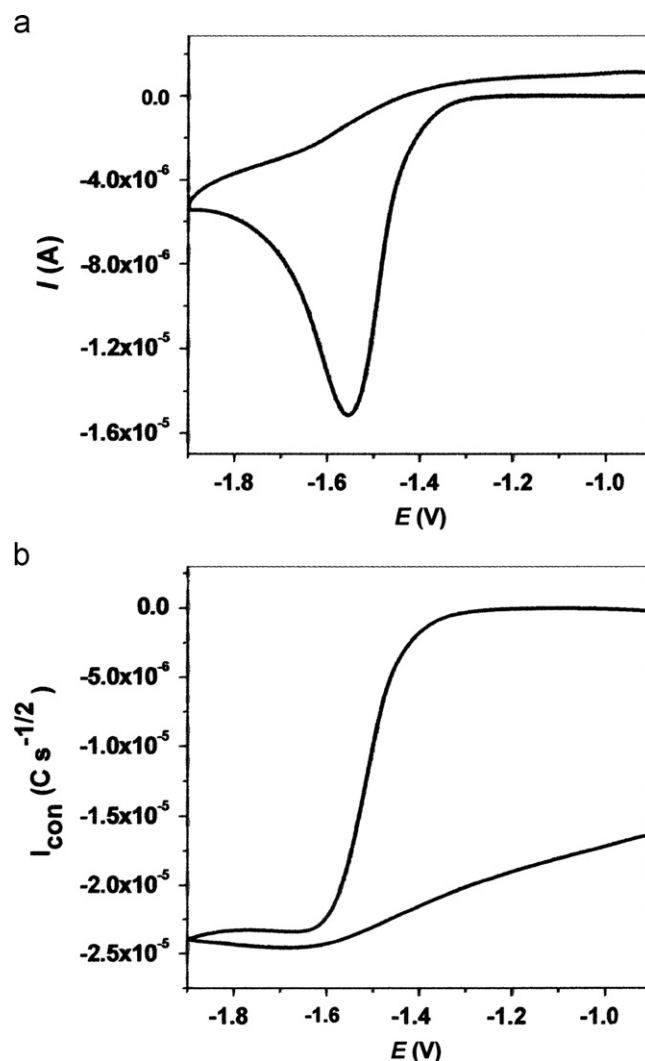
Fig. 1. Cyclic (a) and convoluted cyclic (b) voltammograms of PAT in ACN+0.1 mol L^{-1} TBAP. c^*_{PAT}=5.2×10^{-4} mol L^{-1}. v=0.075 V s^{-1}.

decade, r=0.9939, and $-(0.028 \pm 0.002)$ V/decade, r=0.9961, respectively. This behavior allows inferring a complex electrode process with chemical/electrochemical reaction/s coupled to the initial electron transfer reaction [27].

Wasicki et al. [22] proposed that the PAT electro-reduction mechanism in aqueous buffer solutions is one of the ECE types, where E and C represent electron transfer and chemical reactions, respectively. Moreover, these authors proposed that the chemical reaction was a protonation step between two single-electron transfer reactions. However, experimental variations of $E_{p,c}$ vs. log v, and $E_{p,c}$ vs. log c^*_{PAT} found by us in a non-aqueous medium do not match neither the diagnostic criteria theoretically expected for an ECE mechanism [29,30] nor for electrodimerization reactions [31,32].

On the other hand, convoluted cyclic voltammograms showed that the convoluted current (I_{con}) did not return to zero when the direction of potential sweep was reversed (Fig. 1b), which is a characteristic behavior of redox process with chemical reaction/s followed up to the initial electron transfer [27,33]. In addition, plots of E vs. log $[(I_{L,con}-I_{con})/I]$ were linear, with an average slope of 0.062 ± 0.001 V/decade (r=0.9998) in the range of v from 0.025 to 0.200 V s^{-1}, being this slope close to that theoretically expected for a redox process with the exchange of one electron (n=1), i.e., 0.0592 V/decade at 25 °C [27,33]. From the average

limiting convoluted current ($I_{L,con}$), a value for the PAT diffusion coefficient (D_{PAT}) of $(2.1 \pm 0.1) \times 10^{-5} \, cm^2 \, s^{-1}$ was obtained (assuming $n=1$) through the following equation, which is valid for different reaction mechanisms [33]:

$$I_{L,con} = n \, F \, A \, c^*_{PAT} \, D^{1/2}_{PAT} \qquad (1)$$

being F the Faraday constant, and the other terms were previously defined.

3.1.2. Controlled potential bulk electrolysis

Controlled potential electrolysis was carried out at $E = -1.79 \, V$ during 45 min. Cyclic voltammograms recorded during the electrolysis showed a pronounced diminution in the PAT reduction peak and the development of an oxidation peak, centered at about 1 V (Fig. 2). This peak would correspond to the oxidation of product/s of PAT reduction.

The curve I vs. t at relatively short times (about 100 s) was used to extract the electron number exchanged in the reduction process [34]. Thus, we used the combination of the following equations for the current and the charge (Q) to determine the number of electrons exchanged in the electrode process:

$$I(t) = I(0)\exp(-pt) \qquad (2)$$

and

$$Q(t) = Q(0)[1 - \exp(-pt)] \qquad (3)$$

where $I(0)$ is the current at $t=0$, $Q(0)=nFVc^*_{PAT}$ and $p=m_oA/V$, being m_o the mass transfer coefficient and V the solution volume. For short times, $Q(t)$ can be expressed as:

$$\ln Q \, (t) = \ln Q \, (0) + \ln p + \ln t \qquad (4)$$

Then, n is calculated through the combination of the intercept and the slope of linear plots of ln Q vs. ln t and ln $I(t)$ vs. t, respectively. An average value of $n=(1.07 \pm 0.02)$ was obtained from three replicated measurements. This value is in a good agreement with the n value inferred from slopes of E vs. log $[(I_{L,con}-I_{con})/I]$ plots of the convoluted cyclic voltammograms. On the other hand, an average value of $n=1.1 \pm 0.2$ was obtained from
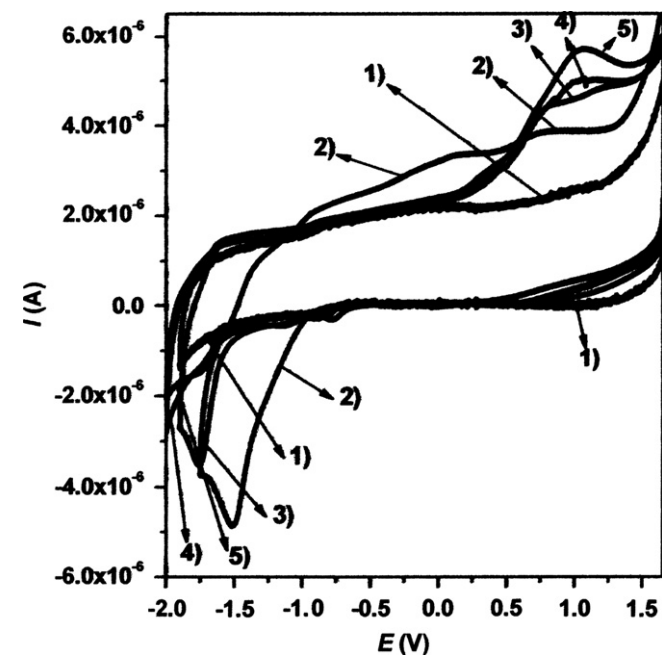
the experimental charge ($Q=1.05 \pm 0.02$) C obtained by integration of the complete $I-t$ transients, in agreement with n obtained from short time transients.

After performing the controlled potential electrolysis, the reaction product was separated from the solvent by evaporation. Then, it was dissolved in a water+dichloromethane (1:1) mixture and transferred to a separator funnel in order to eliminate the supporting electrolyte. The aqueous phase was discarded. Finally, the organic solvent was eliminated by evaporation and the product was dissolved in ACN for recording the UV–vis and IR spectra.

UV–vis spectra recorded before and after performing the controlled potential electrolysis showed that the electro-reduction product presents an absorption band at $\lambda=277 \, nm$ (only 2 nm higher than PAT). This behavior indicates that the PAT chromophore group would not be affected by the electro-reduction. IR spectra of PAT and the electro-reduction product are shown in Fig. 3. The band at $1631 \, cm^{-1}$ (Fig. 3a) can be assigned to the C=O stretching of the ketone group presents in PAT chemical structure (Scheme 1). It is known that the C=O group in ketones, aldehydes, carboxylic acids, anhydrides, amides, lactones and lactams shows a strong stretching band in the region between 1540 and 1870 cm^{-1} [35,36]. In addition, the bands at
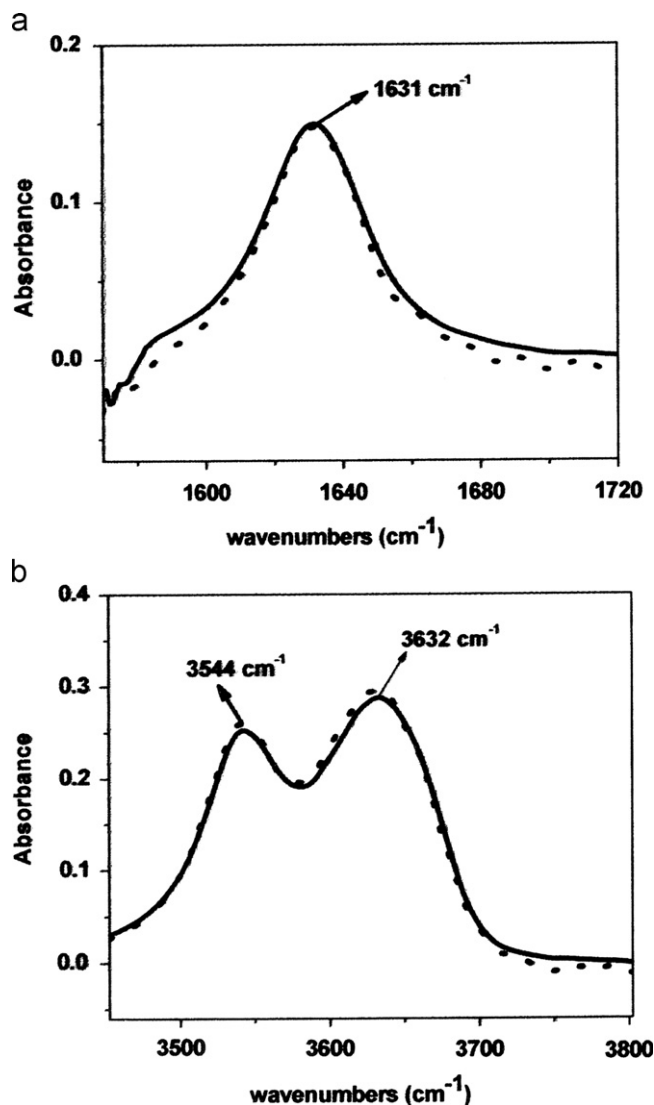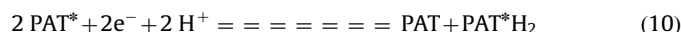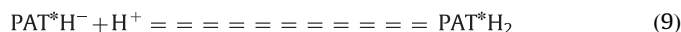
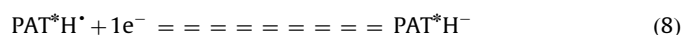**Fig. 3.** IR spectra recorded before (solid line) and after (dotted line) performing the controlled potential electrolysis.

Fig. 2. Cyclic voltammograms of the ACN+0.1 mol L^{-1} NaClO$_4$ (1) and ACN+0.1 mol L^{-1} NaClO$_4$+PAT a different electrolysis times: 2) 0; 3) 15; 4) 30 and 5) 45 min. Initial concentration of PAT, $c^*_{PAT}=3.47 \times 10^{-4}$ mol L^{-1}. $v=0.050$ V s^{-1}.

3544 and 3632 cm^{-1} (Fig. 3b) can be assigned to O–H stretching vibrations of the alcohol group presents in the PAT chemical structure. It is also known that the −OH group in alcohols presents a strong absorption in the region from 3610 to 3640 cm^{-1} and from 3200 to 3600 cm^{-1}, depending on whether the alcohol is a monomer or forming a hydrogen bond, respectively [36]. This clearly shows that the same functional groups are present in the chemical structure of PAT and its electro-reduction product.

Based on these results, and knowing the product of the PAT chemical reduction [23] and the PAT biosynthetic mechanism [11], we propose the following reaction mechanism in neutral medium:

$$PAT^* ===== PAT \tag{5}$$

$$PAT^* + 1e^- ===== PAT^{*-\bullet} \tag{6}$$

$$PAT^{*-\bullet} + H^+ ======= PAT^*H^\bullet \tag{7}$$

$$PAT^*H^\bullet + 1e^- ========= PAT^*H^- \tag{8}$$

$$PAT^*H^- + H^+ ============= PAT^*H_2 \tag{9}$$

$$2\,PAT^* + 2e^- + 2\,H^+ ======= PAT + PAT^*H_2 \tag{10}$$

which involves the exchange of one electron per mole of electrolyzed substance in good agreement with results previously discussed.

PAT* and PAT are the aldehyde and hemiacetal forms of patulin, respectively (Scheme 1). It is well known that both forms are in equilibrium in solution (Eq. (5)) [37]. PAT^{*-} is the radical anion of PAT* (Eq. (6)), which is then protonated to give the corresponding radical, PAT*H$^-$ (Eq. (7)), which is more easily reduced than the starting compound generating the corresponding anion (Eq. (8)). Finally, the PAT*H$^-$ is protonated to give the final product, PAT*H$_2$ (Eq. (9)). The chemical structure of PAT*H$_2$ corresponds to E-ascladiol which would be the most likely product of the electrochemical reduction of PAT. Source of proton for the protonation reactions could be residual water as well as the solvent itself. It has been discussed that ACN can be an active proton donor, starting from the fact that the pKa of ACN is quite similar to that of water (when measured in dimethylsulfoxide) [38]. Thus, considering the great difference in the amount of solvent molecules compared with the residual water would be highly probable that ACN is acting as a proton donor in the protonation reactions (Eqs. (7) and (9)).

Based on this mechanistic proposal, we generated theoretical cyclic voltammograms using the DigiSim® Software for different scan rates and substrate bulk concentrations (c^*) using the CECEC mechanism represented by Eqs. (5)–(9). From the theoretical voltammograms, it was analyzed the dependence of $E_{p,c}$ with both scan rate and c^*. Therefore, it was found $\partial E_{p,c}/\partial \log v = -(0.028 \pm 0.001)$ V/decade and $\partial E_{p,c}/\partial \log c^* = -(0.020 \pm 0.001)$ V/decade, which are in a good agreement with the experimental values found for these dependences (see above).

3.2. Acidic medium

We also studied the effect of the addition of different aliquots of TFA on the PAT voltammetric responses. Therefore, Fig. 4 shows cyclic voltammograms of PAT at $c^*_{PAT} = 4.00 \times 10^{-4}$ mol L^{-1}, without and with the addition of different aliquots of TFA. The TFA bulk concentration (c^*_{TFA}) was varied from 0 to 1.23×10^{-3} mol L^{-1}. The reduction peak of PAT begins to unfold in two peaks as the TFA concentration increases until the acid concentration was approximately two times higher than c^*_{PAT}, where only one cathodic peak was defined centered at about $E_{p,c} = -1.37$ V. The addition of the

TFA produced a shift of the PAT reduction peak at about 0.200 V lesser negative than that obtained in the absence of the acid, and an increase in the current intensity of about 20–22%. The cathodic peak can be assigned to the electro-reduction of protonated PAT (PATH$^+$) [39]. The variation of $I_{p,c}$ of PAT and PATH$^+$ with the ratio between TFA and PAT concentrations (c^*_{TFA}/c^*_{PAT}) is shown in Fig. 5. The $I_{p,c}$ of PATH$^+$ increases up to reach a practically constant value for $c^*_{TFA}/c^*_{PAT} \geq 2$. Moreover, plots of $I_{p,c}$ vs. $v^{1/2}$ for cyclic voltammograms of PATH$^+$ were also linear, showing that the electrode process is diffusion controlled.
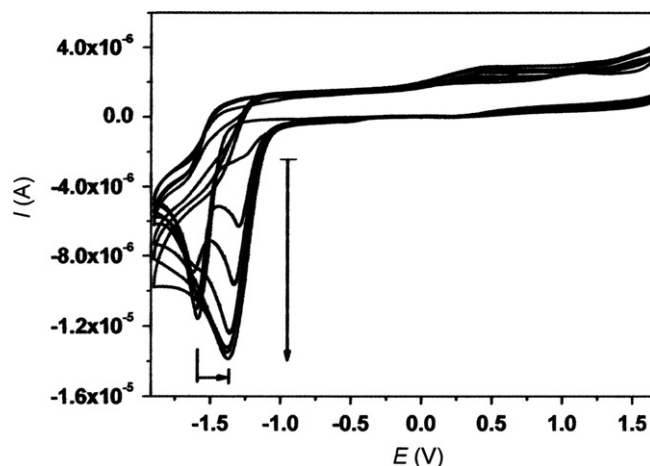

Fig. 4. Cyclic voltammograms of PAT in ACN+0.1 mol L^{-1} TBAP in the absence and in the presence of different aliquots of TFA. $c^*_{PAT} = 4.0 \times 10^{-4}$ mol L^{-1}. c^*_{TFA} was varied from 0 to 1.23×10^{-3} mol L^{-1}. $v = 0.050$ V s^{-1}. Vertical and horizontal arrows indicate the increase in the current, and the shift of the PAT electro-reduction peak at less cathodic potentials, respectively, as the TFA concentration increases.
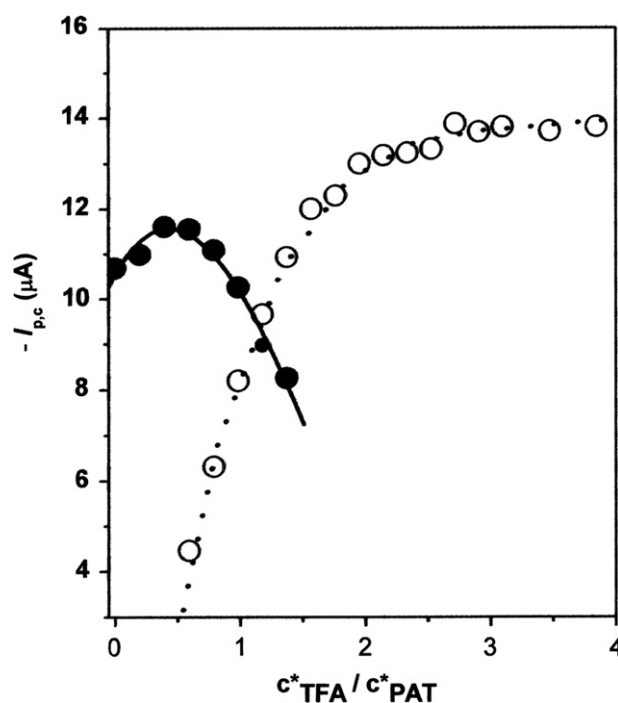

Fig. 5. Variation of the cathodic peak currents of cyclic voltammograms of PAT and PATH$^+$ on the ratio between TFA and PAT concentrations. (●) $I_{p,c,PAT}$, and (o) $I_{p,c,\ PATH+}$. $c^*_{PAT} = 4.0 \times 10^{-4}$ mol L^{-1}. $v = 0.050$ V s^{-1}.

3.3. Voltammetric measurements in the presence of HMF

We also studied the electrochemical behavior of HMF in ACN+0.1 mol L^{-1} TBAP at GC electrodes, in order to analyze the probable interference of HMF in the determination of PAT. HMF shows a single reduction peak centered at $E_{p,c} = -1.875$ V vs. SCE when the potential is swept from 1.650 V to -2.225 V. Cyclic and SW voltammograms were reproducible when a waiting time of 30 s was applied at 1.650 V. No anodic peak was observed in cyclic voltammograms when reversing the direction of potential sweep, showing a complex HMF reduction mechanism, with chemical/s or electrochemical/s reactions coupled to the initial electron transfer process [27]. Plots of $I_{p,c}$ vs. $v^{1/2}$ and net peak currents ($I_{p,n}$) vs. $f^{1/2}$ were linear, showing a diffusion control for the electrode process. Moreover, a plot of $I_{p,c}$ vs. c^*_{HMF} was linear in the range from 3.4×10^{-4} to 2.3×10^{-3} mol L^{-1} (slope$= -0.0186 \pm 0.0009$ A mol^{-1}L, $r=0.9954$). Cyclic and SW voltammograms of HMF in presence of PAT showed that HMF does not interfere in the electrochemical determination of PAT. A separation between PAT and HMF cathodic peak potentials of about 0.325 V was obtained, even when 2.4 times higher was c^*_{HMF} than c^*_{PAT} (Fig. 6). The addition of TFA to the reaction medium produced on the HMF reduction peak the same effect that on the PAT reduction peak; i.e., a shift of about 0.200 V at less cathodic potentials for the ratio $c^*_{TFA}/c^*_{HMF} \geq 2$.

Fig. 6. a) Cyclic and b) SW voltammograms of a mixture of PAT+HMF in ACN+0.1 mol L^{-1} TBAP at a GC electrode. $c^*_{PAT} = 4.0 \times 10^{-4}$ mol L^{-1}. $c^*_{HMF} = 9.8 \times 10^{-4}$ mol L^{-1}. $v = 0.050$ V s^{-1}.

3.4. Square wave voltammetry: quantitative determination of PAT

3.4.1. Commercial reagent

SWV is an effective and rapid electroanalytical technique with well-established advantages, including good discrimination against background currents and low detection limits [40,41]. Based on results obtained in Section 3.3, we infer that SWV should be a good electroanalytical technique for the simultaneous quantification of PAT and HMF in real samples. Therefore, SW voltammograms of PAT were recorded in ACN+0.1 mol L^{-1} TBAP, in the absence and in the presence of TFA, for the ratio $c^*_{TFA}/c^*_{PAT} \geq 2$. Plots of the net peak current ($I_{p,n}$) as a function of $f^{1/2}$ were linear in the f range from 10 to 100 Hz ($r=0.9987$ and $r=0.9985$ in the absence and in the presence of TFA, respectively), also showing a diffusion control for the electrode process.

Linear dependences between $I_{p,n}$ and PAT concentration were found in the concentration range from 7.0×10^{-7} to 2.2×10^{-5} mol L^{-1} and from 3.0×10^{-7} to 2.2×10^{-5} mol L^{-1} in the absence and in the presence of TFA, respectively. The calibration curves obtained at $f=10$ Hz (average values of three replicate measurements) can be represented by least-squares procedures as:

$$I_{p,n}(A) = (2.2 \pm 0.4) \times 10^{-8} + (3.45 \pm 0.05) \times 10^{-2} \; c^*_{PAT} \; (\text{mol L}^{-1}) \quad r = 0.9981 \quad (11)$$

and

$$I_{p,n}(A) = (7 \pm 2) \times 10^{-9} + (3.7 \pm 0.1) \times 10^{-2} \; c^*_{PATH^+} \; (\text{mol L}^{-1}) \quad r = 0.9913 \quad (12)$$

from SW voltammograms recorded in the absence and in the presence of TFA, respectively.

In spite of the sensibility is practically the same in both reaction media, the lowest concentration values measured experimentally for a signal to noise ratio of 3:1 were 7×10^{-7} mol L^{-1} (107 ppb), and 3×10^{-7} mol L^{-1} (45 ppb) in the absence, and in the presence of TFA, respectively, showing the convenience of performing the quantification of PAT under acidic condition.

Based on these results, the detection limit obtained in the presence of TFA is slightly lower than the maximum value allowed by international organizations, i.e. 50 ppb [13]. Therefore, these results enable us to propose this electroanalytical methodology as a rapid screening method to infer the presence of PAT in juice samples.

3.4.2. Apple juices

As previously indicated in Section 2.1, the extraction procedure was conducted firstly on two samples of juice obtained from fresh apples ("cloudy apple juice"). One of these samples was spiked with a known amount of PAT, i.e., 1.29×10^{-5} mol L^{-1}. Both samples were dissolved in the supporting electrolyte solution (ACN+0.1 mol L^{-1} TBAP) and cyclic voltammograms were performed in the potential range from 1.650 to -1.560 V. For these samples it was not necessary to add TFA to the reaction medium considering that the matrix of juice itself has acid components, i.e., ascorbic and citric acids, in an enough amount to perform the measurements under the $c^*_{acid}/c^*_{PAT} \geq 2$ condition. Any voltammetric peak was observed for the non-spiked sample solution. This result shows that other compounds, which are likely extracted with PAT, are not electroactive in the potential range studied (results no shown). However, a cyclic voltammogram recorded in the same potential range on the sample solution which had previously been spiked with the mycotoxin showed one reduction peak in the potential region of discharge of PATH$^+$. Therefore, SWV and the standard additions method were used to calculate the PAT percent recovery. The linear regression found between the corresponding $I_{p,n}$ and added PAT known
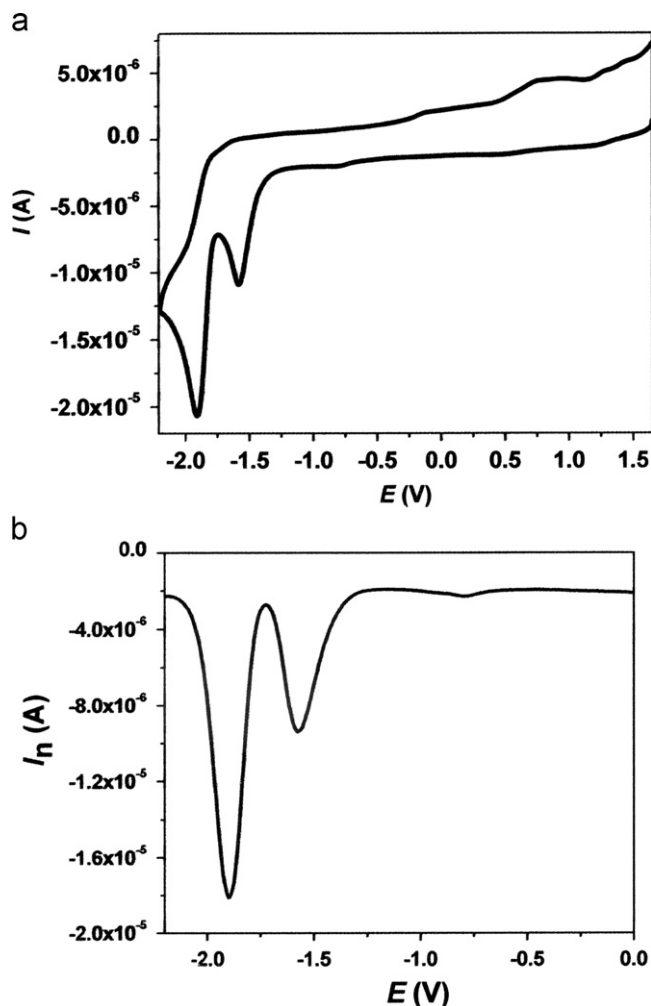
concentrations can be expressed as:

$$I_{p,n} = -(3.2 \pm 0.42) \times 10^{-7} - (3.8 \pm 0.23) \times 10^{-2}$$
$$\times c^*_{PATH^+} \quad r = 0.9930 \tag{13}$$

where $I_{p,n}$ and $c^*_{PATH^+}$ are expressed in A and mol L^{-1}, respectively. Values of $I_{p,n}$ were the average of measurements performed in triplicate (see experimental section). From the relationship between the intercept and the slope of Eq. (13), a recovery percent of 66% was calculated. This relatively low percent recovery can be explained considering that it is known that PAT reacts with some components of the apple juice, such as proteins and amino acids [6,11,42], giving covalent adducts which were not extracted with ethyl acetate. In addition, considering that this was a first approach to the determination of PAT in real matrices, apple juices obtained in our laboratory were not treated with pectinase enzymes, as suggested for the determination of PAT in this type of matrices [16,43]. Moreover, different aliquots of HMF were added to the extract spiked with PAT. Two well-defined reduction peaks were observed by both CV and SWV, even when the HMF concentration was two times higher than that of PAT. The HMF reduction peak appeared at potentials about 0.315 V more negative than the PAT reduction peak (results no shown). Furthermore, the percent recovery obtained for PAT in the presence of HMF was the same as that obtained in the absence of HMF.

From a practical point of view, it is much important to perform analysis of PAT in commercial apple juices. Therefore, a similar procedure to that described for analyzing fresh apple juice ("cloudy apple juice") was applied to analyze commercial apple juice ("clear apple juice"). Therefore, two samples of these juices were studied. One of them was spiked with a known amount of PAT, i.e. 1.29×10^{-5} mol L^{-1}. The composition of the commercial juice stated by the manufacturer was: water, 50% concentrated juice, corn sirup of high fructose, sugar, citric acid, ascorbic acid, and flavoring. Two SW voltammograms of these extracts are shown in Fig. 7. One of them was obtained from the commercial juice without the addition of the mycotoxin, and the other one recorded from the extract which had previously been spiked with PAT. For the first case, the SW voltammogram showed a single reduction peak, with a $E_{p,c}$ at -1.85 V, which can be assigned to the reduction of HMF that is present in commercial juices as a result of the Maillard reaction, which may occur during processing (particularly, at high temperatures) and/or storage of juices, considering that they are rich in

carbohydrates and proteins [44,45]. The SW voltammogram recorded from the extract which had previously been spiked with PAT showed two reduction peaks at $E_{p,c} = -1.51$ V and -1.85 V, corresponding to the reduction of PATH$^+$ and HMFH$^+$, respectively. This shows that the HMF is extracted with PAT, and their reduction peaks are sufficiently separated, allowing the individual determination of each of them (Fig. 7). Then, SWV and the standard additions method were used to determine the percent recovery of PAT. The linear regression between $I_{p,n}$ vs. c^*_{PAT} can be expressed as:

$$I_{p,n} = -(3.1 \pm 0.3) \times 10^{-7} - (2.9 \pm 0.15) \times 10^{-2}$$
$$\times c^*_{PATH^+} \quad r = 0.9988 \tag{14}$$

where $I_{p,n}$ and $c^*_{PATH^+}$ are expressed in A and mol L^{-1}, respectively. Values of $I_{p,n}$ were the average of measurements performed in triplicate (see experimental section). It was obtained a PAT concentration of $(1.1 \pm 0.16) \times 10^{-5}$ mol L^{-1} from the relationship between the intercept and the slope of Eq. (14), which corresponds to a recovery percent of 84% with a RSDR=14%. Recovery obtained is much higher than that previously obtained for fresh juices. Therefore, a calibration curve was constructed from the extracts of ethyl acetate using very low PAT concentrations, which were close to those values allowed by the international law. The calibration curve was linear in the PAT concentration range from 3×10^{-7} to 1.3×10^{-5} mol L^{-1} (ten points were taken into account, which were the average of three replicated measurements), with a slope of $-(4.96 \pm 0.07) \times 10^{-2}$ A mol^{-1} L, $r=0.9954$. The lowest PAT concentration measured for a signal to noise ratio of 3:1 was 3×10^{-7} mol L^{-1} (45 ppb), in agreement with the value found for commercial reagent solutions (Section 3.4.1.).

On the other hand, SWV and the standard additions method were also used to determine the HMF concentration in the commercial juice. Therefore, the linear regression between $I_{p,n}$ vs. $c^*_{HMFH^+}$ can be expressed as:

$$I_{p,n} = -(1.7 \pm 0.15) \times 10^{-6} - (2.9 \pm 0.15) \times 10^{-2}$$
$$\times c^*_{HMFH^+} \quad r = 0.9972 \tag{15}$$

where $I_{p,n}$ and $c^*_{HMFH^+}$ are expressed in A and mol L^{-1}, respectively. Values of $I_{p,n}$ were the average of measurements performed in triplicate (see experimental section). It was obtained a HMF concentration of $(7.0 \pm 0.98) \times 10^{-5}$ mol L^{-1} (8.0 ppm) from the relationship between the intercept and the slope of Eq. (15), assuming a percent recovery close to that found for PAT. This value is within the range allowed by international laws. Thus, the International Federation of Fruit Juice Processors (IFFJP) recommends a maximum concentration of HMF in fruit juices between 5 and 10 ppm, and 25 ppm in concentrated juices [46]. In addition, as far as we know, only one report is found in literature related to the electrochemical reduction of HMF and its application to the analysis of honey samples [47].

We consider that results found show that the electroanalytical methodology developed is satisfactory for screening procedures.

4. Conclusions

The electrochemical reduction of patulin mycotoxin was studied for the first time in a non-aqueous reaction medium. The E-ascladiol is proposed as the more likely reaction product. Results found compared with those few reported in literature indicate that the patulin electrochemical reaction mechanism is different in non-aqueous and aqueous media. The electrochemical reduction of 5-hydroxymethylfurfural, the main interference in the determination of patulin in apple products, was also studied. Both electroreduction peaks of patulin and 5-hydroxymethylfurfural were shifted at less cathodic potentials in the presence of trifluoroacetic acid. In addition, the separation between the reduction peaks of
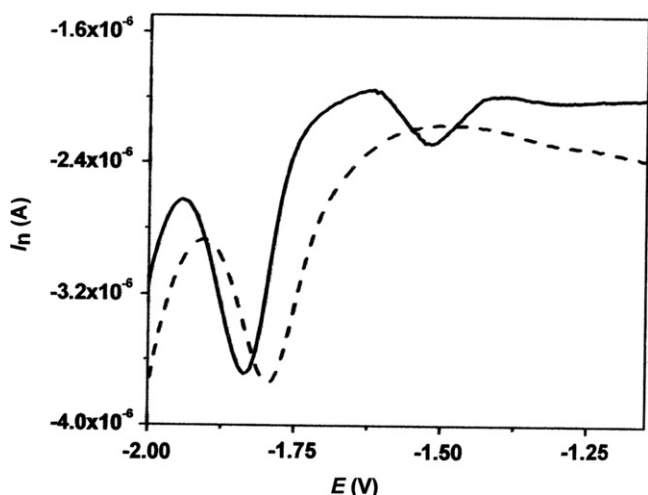

Fig. 7. SW voltammograms of extracts of commercial juices ("clear apple juice") in ACN+0.1 mol L^{-1} TBAP solution not contaminated (dotted line) and when it had previously been spiked with PAT (solid line). $c^*_{PAT} = 1.29 \times 10^{-5}$ mol L^{-1}. $f=10$ Hz, $\Delta E_{sw}=0.025$ V, $\Delta E_s=0.005$ V.

patulin and 5-hydroxymethylfurfural was good enough to allow simultaneous determination of both substrates.

The combination of square wave voltammetry and the standard additions method is proposed as an alternative analytical method for a rapid screening of patulin and 5-hydroxymethylfurfural in apple juices.

Acknowledgments

References

[1] L. González, J.M. Soriano del Castillo, in: J.M. Soriano del Castillo (Director-Coordinador), Micotoxinas en Alimentos, Ediciones Díaz de Santos, Spain, 2007, (Chapter 12).
[2] L.L. Wallen, A.J. Lyons, T.G. Pridham, J. Antibiot. 33 (1980) 767–772.
[3] A. Sant'Ana, A. Rosenthal, P. Rodríguez de Massaguer, Food Res. Int. 41 (2008) 441–568.
[4] A.M. Cheraghali, H.R. Mohammadi, M. Amirahmadi, H. Yazdanpanah, G. Abouhossain, F. Zamanian, M.G. Khansari, M. Afshar, Food Control 16 (2005) 165–167.
[5] M.E. Iha, M. Sabino, J. AOAC Int. 89 (2006) 139–143.
[6] R. Fliege, M. Metzler, Chem. Res. Toxicol. 13 (2000) 373–381.
[7] A. Ritieni, J. Agric. Food Chem. 51 (2003) 6086–6090.
[8] A. Ciegler, R.F. Vesonder, L.K. Jackson, Appl. Environ. Microbiol. 33 (1997) 1004–1006.
[9] R. Mahfoud, M. Maresca, N. Germy, J. Fanzine, Toxicol. Appl. Pharmacol. 181 (2002) 209–218.
[10] G. Selmanoglu, Food Chem. Toxicol. 12 (2006) 2019–2024.
[11] M.M. Moake, O. Padilla-Zakour, R.W. Worobo, Compr. Rev. Food Sci. Food Saf. 1 (2005) 8–21.
[12] International Agency for Research on Cancer (IARC), 2006, available at: ⟨http://www.iarc.fr⟩.
[13] United States Food and Drug Administration, available at: ⟨http://www.fda.gov/Food/FoodSafety/FoodContaminantsAdulteration/NaturalToxins/ucm212520.htm⟩.
[14] Official Journal of the European Union, Comission Regulation (EC) No. 1881/2006 of 19 December 2006, Setting Maximum Levels For Certain Contaminants in Foodstuffs.
[15] L.S. Jackson, Al-Taher, in: F.R. Barkai, G.N. Paster (Eds.), Mycotoxins in Fruits and Vegetables, Elsevier Inc., San Diego, USA, 2008, p. 76, Chapter 4.
[16] A.R. Brause, M.W. Trucksess, F.S. Thomas, S.W. Page, J. AOAC Int. 79 (1996) 451–455.
[17] G.S. Shephard, N.L. Leggott, J. Chromatogr. A 882 (2000) 17–22.
[18] A. Moukas, V. Panagiotopoulou, P. Markaki, Food Chem. 109 (2008) 860–867.
[19] S.C. Cunha, M.A. Faria, J.O. Fernandes, Food Chem. 115 (2009) 352–359.
[20] M. Richlik, P. Schieberle, Food Chem. 47 (1999) 3749–3755.
[21] R. Tsao, T. Zhou, J. Agric. Food Chem. 48 (2000) 5231–5235.
[22] F. Wasicki, F. Scholz, D. Scheleinitz, Pharmazie 41 (1986) 843–844.
[23] H. Tanabe, T. Suzuki, in: M. Herzberg (Ed.), Procedings of the US–Japan Conference Toxic Microorganisms 1st 1968 Published 1970, pp. 127–128.
[24] S.J. Nunes da Silva, P. Zilles Schuch, C.R. Bernardi, M. Henning Vainstein, A. Jablonski, R.J. Bender, Rev. Bras. Frutic. 29 (2007) 406–409.
[25] R.E. Bracket, E.H. Marth, Z. Lebens, Unters. Forsch 169 (1979) 92–94.
[26] ISO 8128-1, 1st Ed. 1993-07-01, UNBS 2009, ⟨http://members.wto.org/crnattachments/2010/tbt/uga/10_2041_00_e.pdf⟩.
[27] A.J. Bard, L.R. Faulkner, Electrochemical Methods: Fundamentals and Applications, 2nd ed., J. Wiley, New York, 2001.
[28] M.A. Zon, M.B. Moressi, L.E. Sereno, H. Fernández, Bol. Soc. Chil. Quím. 39 (1994) 139–151.
[29] R.S. Nicholson, I. Shain, Anal. Chem. 37 (1965) 178–190.
[30] R.S. Nicholson, I. Shain, Anal. Chem. 37 (1965) 190–195.
[31] C.P. Andrieux, L. Nadjo, J.M. Saveant, J. Electroanal. Chem. 26 (1970) 147–151.
[32] C.P. Andrieux, L. Nadjo, J.M. Saveant, J. Electroanal. Chem. 42 (1973) 223–242.
[33] J.C. Imbeaux, J.M. Saveant, J. Electroanal. Chem. 44 (1973) 169–187.
[34] F.J. Arévalo, P.G. Molina, M.A. Zon, H. Fernández, J. Electroanal. Chem. 619–620 (2008) 46–52.
[35] R.M. Silverstein, G.C. Bassler, T.C. Morril, Spectroscopy Identification of Organic Compounds, 4th ed., J. Wiley & Sons, New York, 1981.
[36] T.W. Solomons, Fundamentals of Organic Chemistry, J. Wiley & Sons, New York, 1982.
[37] J. Mc Murry, Química Orgánica, 7th ed., Cengage Learning Editores S. A., México, 2010.
[38] F.G. Bordwell, Acc. Chem. Res. 21 (1988) 456–463.
[39] M.M. Baizer, in: H. Lund, O. Hammerich (Eds.), Org. Electrochem., 4th ed., Marcel Dekker, Inc., New York, 2001.
[40] J. Osteryoung, J. O'Dea, Square Wave Voltammetry, in: A.J. Bard (Ed.), Electroanal. Chem., vol. 14, Marcel Dekker, New Yord, 1987.
[41] K.B. Oldham, J.C. Myland, Fundamentals and Electrochemical Science, Academic Press, San Diego, CA, 1994.
[42] K. Baert, B.D. Meulenaer, Ch. Kasase, A. Huyghebaert, W. Ooghe, F. Devlieghere, Food Chem. 100 (2007) 1278–1282.
[43] S. MacDonald, M. Long, J. Gilbert, J. AOAC Int. 83 (2000) 1387–1394.
[44] E.M.S.M. Gaspar, A.F.F. Lucena, Food Chem. 114 (2009) 1576–1582.
[45] E. Teixido, O. Nuñez, F.J. Santos, M.T. Galceran, Food Chem. 126 (2011) 1902–1908.
[46] V. Gokmen, J. Acar, J. Chromatogr. A 847 (1999) 69–74.
[47] E.O. Reyes-Salas, J.A. Manzanilla-Cano, M.H. Barceló-Quintal, D. Juárez-Mendoza, M. Reyes-Salas, Anal. Lett. 39 (2006) 161–171.